Precision interferometry for measuring wavefronts of multi-wavelength optical pickups

Zongtao Ge[1*] Takayuki Saito[1], Minoru Kurose[1], Hideo Kanda[1], Kazuhisa Arakawa[1] and Mitsuo Takeda[2]

[1] Fujinon Corporation
1-324, Uetake, Saitama City, Saitama 330-8624, Japan
zongtao-ge@msv.fujinon.co.jp
[2] *Department of Information and Communication Engineering*
the University of Electro-Communications
1-5-1, Chofugaoka, Chofu, Tokyo 182-8585, Japan
takeda@ice.uec.ac.jp

http://www.fujinon.co.jp, http://www.uec.ac.jp/

Abstract: A novel wavefront measurement interferometer is developed that enables the user to evaluate the wavefronts of multi-wavelength optical pickups. In this interferometer, instead of transparent pinholes used in Mach-Zehnder interferometers, reflection dot pinhole mirrors are used to generate reference wavefronts for different wavelengths which make the optical system very flexible and simple compared with those using transparent pinholes. The interferometer is designed to operate at wavelengths of 405nm, 650nm and 780nm over an NA range of up to 0.95, which is very difficult to realize when transparent pinholes are used for generating reference wavefronts. The three-beam problem is solved and the optics of the interferometer is simplified by employing a software filter instead of using spatial filters in the optics of the interferometer. The instrument has an equal optical path length that enables the user to measure pickups with a very short coherence length. A new method by which asymmetric aberration components, such as astigmatic and coma aberrations, can be calibrated by rotating the measured lens with 90 and 180 degrees is proposed and the calibration results are verified by using a high precision reference point source. System accuracy is also evaluated by comparing with the measurement results obtained by commercial Fizeau type interferometer and a good agreement is achieved.

OCIS codes: (120.0120) Instrumentation, measurement, and metrology: Instrumentation, measurement, and metrology;. (120.3180) Instrumentation, measurement, and metrology: Interferometry; (120.5050) Instrumentation, measurement, and metrology: Phase measurement.

References and links

1. Benno H. W. Hendriks, Jean Schleipen, Sjoerd Stallinga and Henk van Houten, "Optical Pickup for blue optical recording at NA=0.85," Opt.l Rev. **8,** 211-213 (2001).
2. Donald K. Cohen, Blake Little, Frank S. Luecke, "Techniques for measuring 1-μm diameter Gaussian beams," Appl. Opt. **23,** 637-640 (1984).
3. E. C. Broockman, L. D. Dickson, and R. S. Fortenberrgy, "Generalization of the Ronchi ruling method for measuring Gaussian beam diameter," Opt. Eng. **22,** 643-647 (1983).
4. Yasuhiro Tanaka and Motonobu Yoshikawa, "Novel measuring technique of optical performance in objective lenses for optical disk systems," Appl. Opt. **31,** 5305-5311 (1992).
5. J. -S. Lee, H. -S. Yang, and J. -W. Hahn, "Wavefront error measurement of high-numerical-aperture optics with a Shack-Hartmann sensor and a point source," Appl. Opt. **46,** 1411-1415 (2007).
6. H. -S. Yang, J. -B. Song, I. -W. Lee, and Y. -W. Lee, "Testing of steep convex aspheric surface with a Hartmann sensor by using a CGH," Opt. Express **14,** 3247-3254 (2006).
7. Timothy L. Pennington, Byron M. Welsh, and Michael C. Roggemann, "Performance Comparison of the Shearing interferometer and the Hartmann wavefront sensor," Proc SPIE **2201,** 508-518 (1994)

#87937 - $15.00 USD Received 28 Sep 2007; revised 20 Nov 2007; accepted 23 Nov 2007; published 2 Jan 2008

8. W.-J. Cho and Seung-Woo Kim, “Stable lateral-shearing interferometer for production-line inspection of lenses,” Opt. Eng. **36,** 896-900 (1997).
9. D. Korwan, “Lateral-shearing interferogram analysis,” Proc. SPIE **0429,** 194-198 (1983).
10. R. N. Smartt and W. Stell, “Theory and application of point-diffraction interferometer,” Jpn. J. Appl. Phys. **14,** 351-356 (1975).
11. R. N. Smartt, “Special application of the point-diffraction interferometer,” Proc. SPIE **192,** 35-40 (1979).
12. B. E. Truax, “A phase measuring radial shear interferometer for measuring the wavefront of compact Disc laser pickups,” Proc. SPIE **661,** 74-82 (1986).
13. R. de la Fuente and E. López Lago, "Mach-Zehnder diffracted beam interferometer," Opt. Express **15,** 3876-3887 (2007).
14. C. R. Mercer and K. Creath, "Liquid-crystal point-diffraction interferometer for wave-front measurements," Appl. Opt. **35,** 1633 (1996).
15. M. Paturzo, F. Pignatiello, S. Grilli, S. De Nicola, and P. Ferraro, "Phase-shifting point-diffraction interferometer developed by using the electro-optic effect in ferroelectric crystals," Opt. Lett. **31,** 3597-3599 (2006).
16. C. L. Koliopoulos, O. Kwon, R. Shagam, J. C. Wyant, and C. R. Hayslett, "Infrared point diffraction interferometer," Opt. Lett. **3,** 118- (1978).
17. G. Harbers, P. J. Kunst, and G. W. R. Leibbrandt, "Analysis of lateral shearing interferograms by use of Zernike polynomials," Appl. Opt. **35,** 6162-6172 (1996).
18. S. Okuda, T. Nomura, K. Kamiya, H. Miyashiro, K. Yoshikawa, and H. Tashiro, "High-Precision Analysis of a Lateral Shearing Interferogram by use of the Integration Method and Polynomials," Appl. Opt. **39,** 5179-5186 (2000).
19. G. Schulz and J. Schwider, "Precise measurement of planeness," Appl. Opt. **6,** 1077 (1967).
20. R. E. Parks, L. Shao, and C. J. Evans, "Pixel-Based Absolute Topography Test for Three Flats," Appl. Opt. **37,** 5951-5956 (1998).
21. B. B. F. Oreb, D. I. Farrant, C. J. Walsh, G. Forbes, and P. S. Fairman, "Calibration of a 300-mm-Aperture Phase-Shifting Fizeau Interferometer," Appl. Opt. **39,** 5161-5171 (2000).
22. M. Born and E. Wolf, *Principles of Optics* (Pergamon press, New York, 1980) p.470.

1. Introduction

With the progress of digital high-resolution television broadcasting, there has been an increasing demand for high-density optical storage systems. Thanks to the invention of a blue laser, optical storage with the density up to 30 to 50GB (for example, HD-DVD and BD) in one optical disk became possible [1]. A future approach will be a multi-wavelength optical pickup that makes previous CD, DVD and BD or HD-DVD compatible. Because a pickup head is a key module in the optical drive, optical components used in the pickup should be strictly inspected. Furthermore, in the process of manufacturing optical pickups for blue laser, the quality of the focused spot beam should be carefully monitored so that the position and the status of the components can be adjusted. In the age of CD and DVD, instruments for measuring the intensity distribution of the focused spot are widely used for this purpose [2-3]. Although these instruments are especially useful for the adjustment and inspection of optical pickups, it is difficult to obtain enough diagnostic information, such as wavefront aberrations, for improving the quality of the optical components. Tanaka and Yoshikawa proposed a method to calculate wavefront aberration by analyzing the intensity distribution of the focused spot [4]. This analysis is only an estimation of the aberration, and the accuracy is not enough for newly developed high-density optical pickups. Hartmann wavefront sensors are used to evaluate the wavefront quality of the beams but the precision is not satisfactory for current use because of the poor lateral resolution [5-7]. Lateral shearing interferometers are other tools for measuring the wavefront of the optical pickups [8-9]. The wavefront reconstruction in the lateral shearing interferometer is very complicated because a set of differential equations should be solved by numerical method and integration is also necessary. Furthermore, the process requires narrow wavelength band and to separate x and y channels, and the exact value of the shear should be known. Smartt [10-11] proposed a point-diffraction interferometer using transparent pinhole for generating reference wavefront, but this method is computationally intensive and only suitable for low NA test. Radial shearing interferometers in which transparent pinholes are used for reference wavefront generation is effective for measuring wavefront of optical pickups [12]. Most radial shearing

#87937 - $15.00 USD Received 28 Sep 2007; revised 20 Nov 2007; accepted 23 Nov 2007; published 2 Jan 2008

interferometers employing the Mach-Zehnder layout [13] are too complicated to extend the application to multi-wavelength pickups.

In this paper, we describe a new simple Michelson type interferometer named as BA-3 for measuring wavefronts of multi-wavelength optical pickups for CD, DVD, HD-DVD and BD optical Disks. In the developed interferometer, different reflection pinhole mirrors are used to generate reference wavefronts of different wavelengths. The results of measurement of DVD and BD pickups are presented, and the accuracy of the instrument is evaluated by using a standard point source. The results of the measurement of pickup lenses with the newly developed interferometer were found to be in good agreement with those obtained by Fujinon commercial interferometers.

2. Principle

2.1. Reflection pinhole mirror for generating reference wavefront

Generating reference wavefront is the most important subject in wavefront measurement interferometers. Transparent pinholes are usually used to generate reference wavefront in point diffraction interferometers [14-15]. For the same reason, reflection pinhole mirror can also be used for generating reference wavefront. Figure 1 illustrates the reference wavefront generation by using a reflection pinhole mirror. Figure 2 is a SEM image of the reflection pinhole mirror. Theory about transparent pinholes is also applicable to reflection pinholes. Koliopoulos [16] recommended a pinhole size less than or equal to one half of Airy disk. In our system, the sizes of the pinhole mirrors are chosen to be nearly equal to the Airy disk diameters for different wavelengths, because we have found by computer simulation that the pinholes of these sizes guarantee enough performance for our present applications. Using a reflection pinhole mirror has the advantages that the optics can be largely simplified and greatly expands the possibility of interferometer design. Furthermore, the reflection pinhole enables multi-wavelength measurements, which have been difficult with transparent pinholes in the Mach-Zehnder layout interferometers because the path matching is difficult due to chromatic aberrations. Additionally, the system is easy for alignment and adjustment. The main problem using the reflection pinhole mirror for generating reference wavefront is the low SNR because it is difficult to suppress the unwanted reflection from outside the pinhole area to a sufficiently low level. This can be improved by AR coating the pinhole mirror substrate, which reduces reflection from outside the pinhole mirror area while maintaining the high reflection from the pinhole mirror.

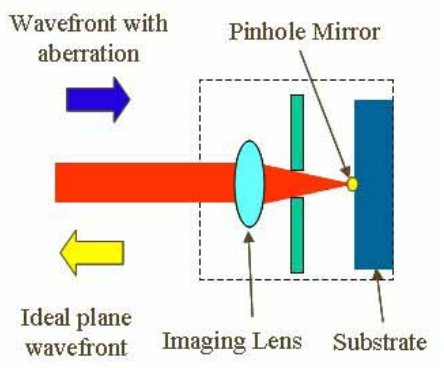

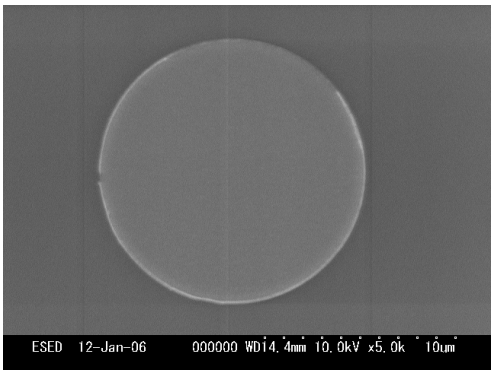

Fig. 1. Pinhole mirror for reference wavefront generation. Fig. 2. SEM image of reflection pinhole mirror.

2.2. Optical design of the interferometer

The optical layout of the interferometer is shown in Fig. 3. In the case of BD (HD-DVD is also applicable) pickup, the wavelength used in the pickup is 405nm. The input beam from the optical pickup passes through a piece of cover plate which simulates the polycarbonate cover layer of an optical disk. After being collimated to a parallel beam by an objective with a high

#87937 - $15.00 USD Received 28 Sep 2007; revised 20 Nov 2007; accepted 23 Nov 2007; published 2 Jan 2008

NA of 0.95, one part of the beam is reflected by a beam splitter BS1 to the reference mirror M1. The beam reflected from M1 then travels back to BS1 and passes through BS1. The other part of the beam passes through BS1 and is input into the blue focusing lens (WLB) which has a negligible aberration. The WLB focuses the beam onto the reflection pinhole mirror B-spot by which the input beam with aberration is converted to an ideal spherical wave front and returns to BS1 after passing through the WLB and converted to ideal plane wavefront. This ideal plane wavefront is then combined with the beam reflected back from M1, and the interferogram of the two beams are observed by a CCD camera B-CCD. In the case of a DVD pickup, a pinhole mirror R-spot and a focusing lens WLR slide into the interferometer for generating ideal spherical wave front. The combined beam is observed by R/IR CCD camera through an R/IR imaging lens. In the case of CD pickup, another pinhole mirror IR-spot and a focusing lens WLIR are moved into the interferometer for generating an ideal spherical wave front. The combined beam is also observed by R/IR CCD camera through a relay lens RLR/IR. The sizes of the pinhole mirrors and the NA of the focusing lenses for the three wavelengths are designed to generate ideal spherical wavefronts for different wavelengths. In the present interferometer, the diameters of the pinhole mirrors are about 4μm for 405nm, 5.5μm for 650nm and 6μm for 780nm, respectively, which are approximately the same sizes as the Airy disk diameters for the individual wavelengths. Alignment optics including a laser source LD, auto-collimating lens CL-A and CCD camera CCD-A is introduced into the system by inserting a mirror M2 so that the inclination of the measured sample and cover plate can be measured and adjusted. The whole system is designed such that chromatic aberration caused by different wavelength is largely reduced. Standard sources with small aberration of three wavelengths are equipped so that a single pickup lens can also be measured. By removing the high NA objective, a parallel beam from the optical pickup can also be evaluated. The developed system is versatile and flexible for various inspection and measurement applications in the development and manufacturing of optical pickups.

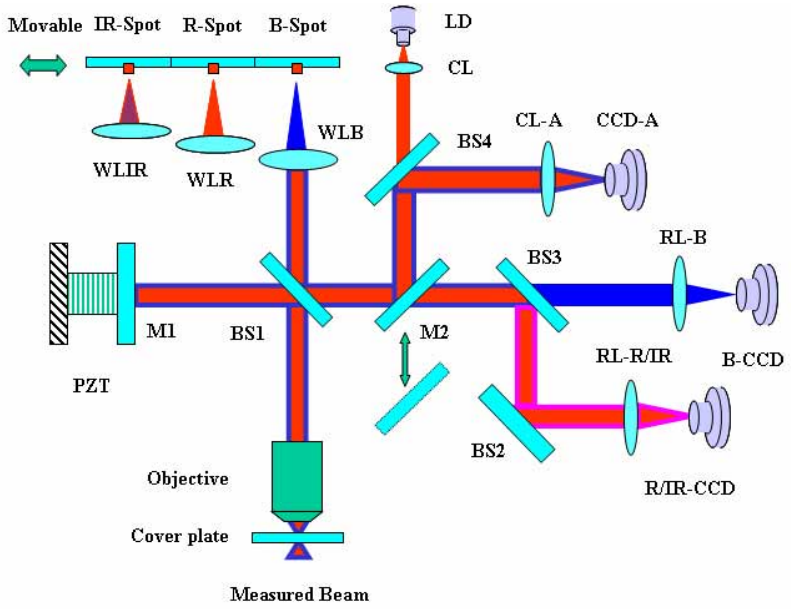

Fig. 3. Optical layout of the interferometer

2.3. Three-beam problem

In typical optical pickups, gratings are used to diffract the beam into a main beam and two tacking beams. These three beams generate an interferogram with high frequency components which may cause a failure in phase unwrapping and high-frequency component errors in fringe analysis. Usually, a spatial filter can be inserted in the imaging path of the

#87937 - $15.00 USD Received 28 Sep 2007; revised 20 Nov 2007; accepted 23 Nov 2007; published 2 Jan 2008

interferometer to filter out the high frequency components. For multi-wavelength applications, the diameter of the spatial filter should be made variable to meet the imaging optics of different wavelengths, which makes the imaging optics complicated and difficult to align. In the developed system, a software filtering method is used to filter out the high frequency component in the phase-shifted interferograms. To reduce filtering calculations, one could, in principle, remove high frequency component errors by using the software filter after the wavefront is reconstructed. In many cases, however, the high frequency component may cause the failure in phase unwrapping process so that wavefront can not be reconstructed.

3. Experiments

3.1. Measurement results

The three-beam errors are evaluated at first. As stated in section 2.3, software filters can be used for reducing high frequency component errors caused by the multi-beam structure of the optical pickups. Shown in Fig. 4 and 5 are an interferogram of three beams of a BD pickup and the 3D image of the reconstructed wavefront where high frequency component errors are observed. Figure 6 is an example of FFT low-pass filter to filter out high frequency components. Figure 7 is the 3D image of the reconstructed wavefront from the interferograms obtained by using the low-pass filter (LPF) shown in Fig. 6. By comparing 3D image of the reconstructed wavefront shown in Fig. 5 and 7, it is observed that the wavefront form is about the same, but errors caused by high frequency components are largely reduced so that the obtained aberration in RMS reduced from 0.076λ to 0.054λ.

Figure 8 and 9 show the interferogram and measurement results when a DVD pickup head is measured. The aberration of the pickup is about 0.042 waves in rms. Figures 10 and 11 show the interferogram and measurement results of parallel beam of an HD-DVD pickup when the objective lens is removed off. Three beam errors are also reduced by using FFT low-pass filter.

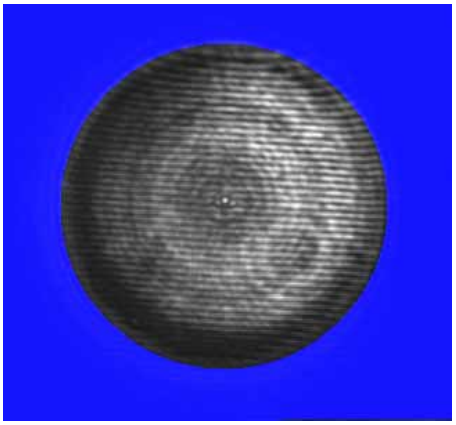

Fig. 4. Interferogram of three beams of a BD pickup

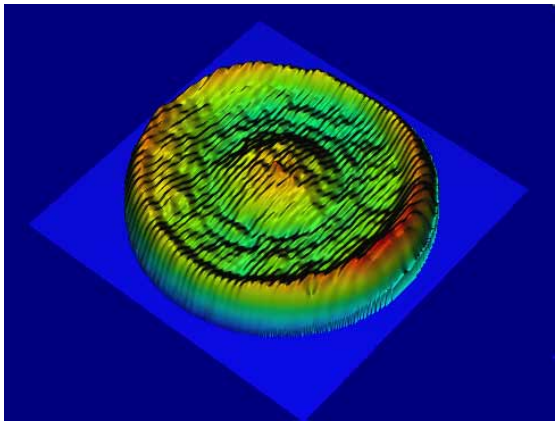

Fig. 5. 3D image of the reconstructed wavefront

#87937 - $15.00 USD Received 28 Sep 2007; revised 20 Nov 2007; accepted 23 Nov 2007; published 2 Jan 2008

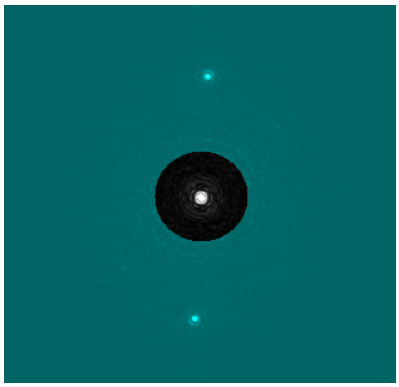

Fig. 6. Example of FFT low-pass filter

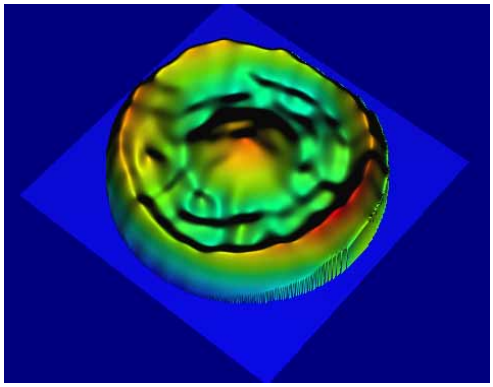

Fig. 7. 3D image of the obtained wavefront after LPF

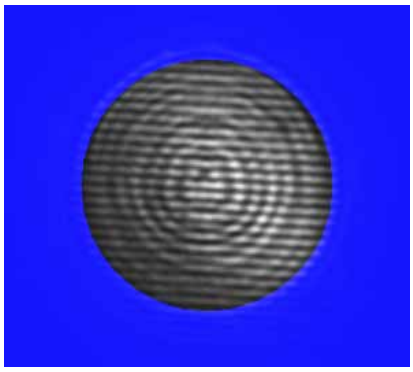

Fig. 8. Interferogram of DVD pickup

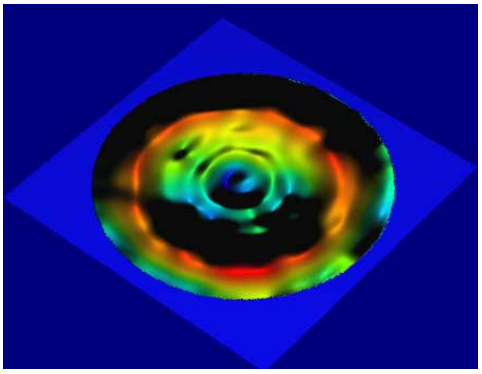

Fig. 9. 3D image of reconstructed wavefront

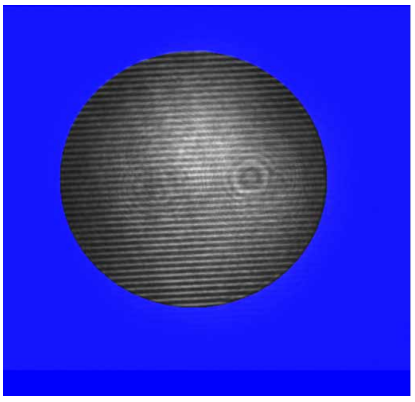

Fig. 10. Interferogram of parallel beam of HD-DVD pickup

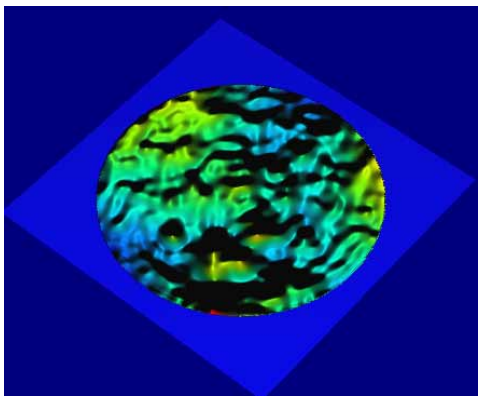

Fig.11. 3D image of reconstructed wavefront

3.2. Comparison with Commercial Interferometer

In order to verify the measurement results of the developed BA-3 interferometer, three BD pickup objective lenses are measured and the measurement results are compared with those obtained by using a Fizeau-type Fujinon V10 interferometer, which is designed to measure objective lenses of BD pickups. Table 1 shows the results of comparison. The results are found to be in good agreement with each other despite that they are obtained by totally different measurement methods.

#87937 - $15.00 USD Received 28 Sep 2007; revised 20 Nov 2007; accepted 23 Nov 2007; published 2 Jan 2008

Table 1, Comparison of resulted wavefronts of BD lenses measured by BA-3 and V-10 (Units in λ)

Sample No. / Items	No.1		No.2		No.3	
	V10	BA-3	V10	BA-3	V10	BA-3
PV	0.438	0.402	0.445	0.402	0.441	0.410
RMS	0.054	0.058	0.054	0.058	0.056	0.056
AS	0.033	0.028	0.016	0.014	0.016	0.016
Coma	0.032	0.034	0.025	0.034	0.024	0.020
SA3	0.004	0.008	0.016	0.008	0.015	0.012

4. System error calibration

4.1. System error calibration using a point source

Several methods can be used for system error calibrations, for example shearing methods [17-18] and the three-surface inter-comparison methods [19-21]. These methods are valuable but the processes are relatively complicated. System error of the developed interferometer is directly calibrated by a standard wavefront generated by using a transparent pinhole with a diameter of 0.532μm. Figure12 illustrates a standard wavefront generation setup used for system error calibration. Figure 13 shows the SEM image of the transparent pinhole formed on a thin glass plate. The pinhole is illuminated by a BD objective lens so that high NA standard wavefront can be obtained. Experiments show that the system RMS errors of the interferometer calibrated by the standard source are AS=0.008λ, Coma=0.001λ, and SA3=0.013λ, respectively.

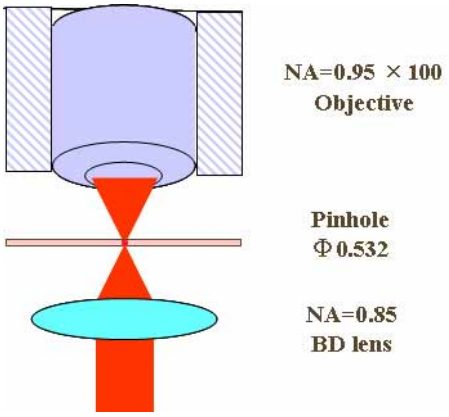

Fig. 12. Standard wavefront generation setup

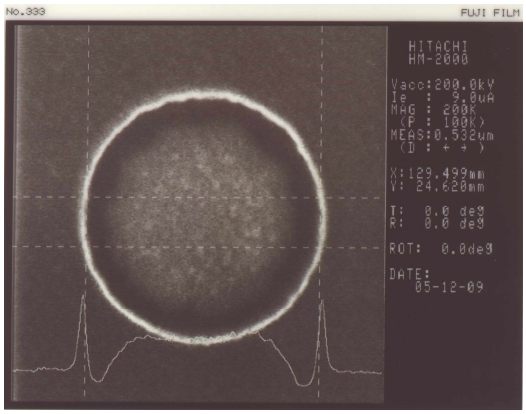

Fig. 13. SEM image of the transparent pinhole

4.2. Asymmetric system error calibration by rotating the measured test lens

We noticed that the wavefront of an optical pickup can be separated into two categories, i.e., one of them are the rotationally symmetric components and the other are rotationally asymmetric components. Asymmetric components of aberration can be obtained by simple computation from wavefront obtained when rotating the measured sample by 90 degrees. This can be used to verify the astigmatism and coma aberrations of system error calibration described in the previous section. Contour images of the reconstructed wavefront obtained when the test sample is rotated are shown in Fig. 14 where the rotations of asymmetric components in the wavefront are obviously observed.

#87937 - $15.00 USD Received 28 Sep 2007; revised 20 Nov 2007; accepted 23 Nov 2007; published 2 Jan 2008

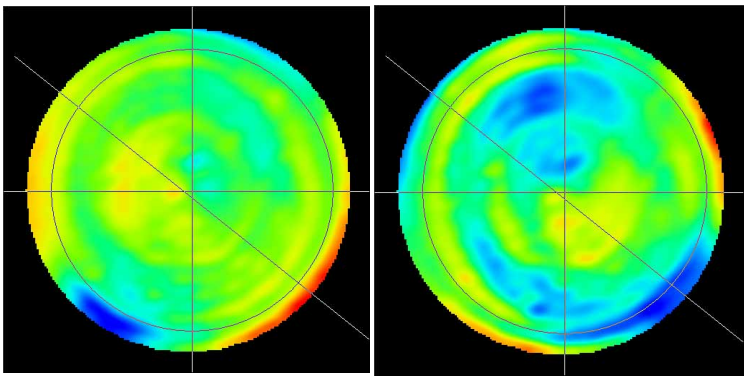

(a) 0degree (b) 90 degrees

(c) 180 degrees (d) 270 degree

Fig. 14. Contour images of the reconstructed wavefront obtained by rotating the test lens

Let $W(\rho, \theta)$, $S(\rho, \theta)$, and $M(\rho, \theta)$ be the wavefronts of the test sample, system error, and measured data, respectively. Here, (ρ, θ) is the pupil coordinate defined in a polar coordinate system.

$$M_{\varphi}(\rho,\theta) = W_{\varphi}(\rho,\theta) + S_{\varphi}(\rho,\theta), \tag{1}$$

where $\varphi = 0^{\circ}, 90^{\circ}, 180^{\circ}, 270^{\circ}, 360^{\circ}$, respectively. Our purpose is to estimate astigmatism and coma aberrations of $W(\rho, \theta)$ and $S(\rho, \theta)$ from the several astigmatism and coma aberrations of $M_{\varphi}(\rho, \theta)$ values measured with the test sample being rotated.

Usually, the astigmatic aberrations of the measured value, the test sample, and the measurement system can be expressed, respectively, by [22]:

$$A_{am}(\rho,\theta) = A_{am}\rho^2 \cos^2(\theta + \varphi_{am}) \tag{2}$$

$$A_{aw}(\rho,\theta) = A_{aw}\rho^2 \cos^2(\theta + \varphi_{aw}) \tag{3}$$

$$A_{as}(\rho,\theta) = A_{as}\rho^2 \cos^2(\theta + \varphi_{as}) \tag{4}$$

We have:

$$A_{am(0)}(\rho,\theta) = A_{aw(0)}(\rho,\theta) + A_{as}(\rho,\theta) \tag{5}$$

#87937 - $15.00 USD Received 28 Sep 2007; revised 20 Nov 2007; accepted 23 Nov 2007; published 2 Jan 2008

$$A_{am(90)}(\rho,\theta) = A_{aw(90)}(\rho,\theta+90) + A_{as}(\rho,\theta) \tag{6}$$

And:

$$\begin{aligned} A_{am(0)}(\rho,\theta) + A_{am(90)}(\rho,\theta) &= A_{aw(0)}\rho^2\cos^2(\theta+\varphi_{aw(0)}) + A_{aw(0)}\rho^2\cos^2(\theta+\varphi_{aw(0)}+90) + 2A_{as}(\rho,\theta) \\ &= 2A_{as}(\rho,\theta) + A_{aw(0)}\rho^2 \end{aligned} \tag{7}$$

$$\begin{aligned} A_{am(0)}(\rho,\theta) - A_{am(90)}(\rho,\theta) &= A_{aw(0)}\rho^2\cos^2(\theta+\varphi_{aw(0)}) - A_{aw(0)}\rho^2\cos^2(\theta+\varphi_{aw(0)}+90) \\ &= 2A_{aw(0)}(\rho,\theta) - A_{aw(0)}\rho^2 \end{aligned} \tag{8}$$

Note that, in Eq. (7) and (8), the term $A_{aw(0)}\rho^2$ becomes the curvature of the wavefront or defocus and only the first term appears as astigmatism aberration. For the astigmatism aberration we have:

$$A_{am(0)}(\rho,\theta) + A_{am(90)}(\rho,\theta) = 2A_{as}(\rho,\theta) \tag{9}$$

$$A_{am(0)}(\rho,\theta) - A_{am(90)}(\rho,\theta) = 2A_{aw(0)}(\rho,\theta), \tag{10}$$

which means the astigmatism aberration of the measurement system is one half the sum of the measured astigmatism aberrations at 0 degree and 90 degrees and that of the test sample is one half the difference of the measured astigmatism aberrations when the test sample is set at 0 degree and rotated by 90 degrees.

For the same reason we can obtain a relationship between coma aberrations of the test sample, the system and those measured when the test sample is set at 0 degree and rotated by 180 degrees:

$$A_{cm(0)}(\rho,\theta) + A_{cm(180)}(\rho,\theta) = 2A_{cs}(\rho,\theta) \tag{11}$$

$$A_{cm(0)}(\rho,\theta) - A_{cm(180)}(\rho,\theta) = 2A_{cw(0)}(\rho,\theta) \tag{12}$$

Where:

$$\begin{cases} A_{cm}(\rho,\theta) = A_{cm}\rho^3\cos(\theta+\varphi_{cm}) \\ A_{cw}(\rho,\theta) = A_{cw}\rho^3\cos(\theta+\varphi_{cw}) \\ A_{cs}(\rho,\theta) = A_{cs}\rho^3\cos(\theta+\varphi_{cs}) \end{cases} \tag{13}$$

From Eq. (9) we have,

$$\begin{aligned} A_{as}(\rho,\theta) &= \frac{A_{am(0)}(\rho,\theta) + A_{am(90)}(\rho,\theta)}{2} \\ &= \frac{A_{am(0)} + A_{am(90)}}{4}\rho^2 + \frac{A_{am(0)}\rho^2\cos 2(\theta+\varphi_{am(0)}) + A_{am(90)}\rho^2\cos 2\left[(\theta+\varphi_{am(0)}) + (\varphi_{am(90)} - \varphi_{am(0)})\right]}{4} \end{aligned} \tag{14}$$

For the same reason, the first defocus term can be ignored and finally we have:

$$A_{as}(\rho,\theta) = \frac{\sqrt{M^2+N^2}\cos^2(\theta+\varphi_{am(0)}+\frac{1}{2}\alpha)}{2}\rho^2 + \frac{\sqrt{M^2+N^2}}{2}\rho^2, \tag{15}$$

where:

#87937 - $15.00 USD Received 28 Sep 2007; revised 20 Nov 2007; accepted 23 Nov 2007; published 2 Jan 2008

$$\begin{cases} M = A_{am(0)} + A_{am(90)} \cos 2(\varphi_{am(90)} - \varphi_{am(0)}) \\ N = A_{am(90)} \sin 2(\varphi_{am(90)} - \varphi_{am(0)}) \\ \alpha = \arctan(\dfrac{N}{M}) \end{cases} \tag{16}$$

From Eq. (10) we have,

$$\begin{aligned} A_{aw}(\rho,\theta) &= \frac{A_{am(0)}(\rho,\theta) - A_{am(90)}(\rho,\theta)}{2} \\ &= \frac{A_{am(0)} - A_{am(90)}}{4}\rho^2 + \frac{A_{am(0)}\rho^2 \cos 2(\theta + \varphi_{am(0)}) - A_{am(90)}\rho^2 \cos 2((\theta + \varphi_{am(0)}) + (\varphi_{am(90)} - \varphi_{am(0)}))}{4} \end{aligned} \tag{17}$$

By ignoring the first term, we have:

$$A_{aw}(\rho,\theta) = \frac{\sqrt{K^2 + N^2}\cos^2(\theta + \varphi_{am(0)} - \frac{1}{2}\beta)}{2}\rho^2 + \frac{\sqrt{K^2 + N^2}}{2}\rho^2 \tag{18}$$

where:

$$\begin{cases} K = A_{am(0)} - A_{am(90)} \cos 2(\varphi_{am(90)} - \varphi_{am(0)}) \\ \beta = \arctan(\dfrac{N}{K}) \end{cases} \tag{19}$$

From Eq. (11) we have,

$$\begin{aligned} A_{cs}(\rho,\theta) &= \frac{A_{cm(0)}(\rho,\theta) + A_{cm(180)}(\rho,\theta)}{2} \\ &= \frac{\sqrt{P^2 + Q^2}\cos(\theta + \varphi_{cm(0)} + \gamma)}{2}\rho^3 \end{aligned} \tag{20}$$

where:

$$\begin{cases} P = A_{cm(0)} + A_{cm(180)} \cos(\varphi_{cm(180)} - \varphi_{cm(0)}) \\ Q = A_{cm(180)} \sin(\varphi_{cm(180)} - \varphi_{cm(0)}) \\ \gamma = \arctan(\dfrac{Q}{P}) \end{cases} \tag{21}$$

From Eq. (12) we have,

$$\begin{aligned} A_{cw}(\rho,\theta) &= \frac{A_{cm(0)}(\rho,\theta) - A_{cm(180)}(\rho,\theta)}{2} \\ &= \frac{\sqrt{T^2 + Q^2}\cos(\theta + \varphi_{cm(0)} - \varepsilon)}{2}\rho^3 \end{aligned} \tag{22}$$

where:

$$\begin{cases} T = A_{cm(0)} - A_{cm(180)} \cos(\varphi_{cm(180)} - \varphi_{cm(0)}) \\ \varepsilon = \arctan(\dfrac{Q}{T}) \end{cases} \tag{23}$$

According to Eq. (15), (18), (20) and (22), calculation macros can be obtained and are shown in Table 2 by which astigmatism and coma aberrations of the test sample and the measurement system can be estimated separately.

#87937 - $15.00 USD Received 28 Sep 2007; revised 20 Nov 2007; accepted 23 Nov 2007; published 2 Jan 2008

Table 2. Estimation of RMS astigmatism and coma aberrations using data obtained by rotating the test sample

1	Items	0Deg	90Deg	180Deg	270Deg	360Deg	
2	AS-RMS	0.0323	0.0323	0.0323	0.0323	0.0323	
3	AS-ANGLE	39.20	123.10	43.20	107.40	39.20	
4	COMA-RMS	0.0138	0.0138	0.0138	0.0138	0.0138	
5	COMA-ANGLE	135.60	45.10	322.20	201.60	129.80	
6	AS of System	$A_{am(0)}(\rho, \theta)+A_{am(90)}(\rho, \theta)$	$A_{am(90)}(\rho, \theta)+A_{am(180)}(\rho, \theta)$	$A_{am(180)}(\rho, \theta)+A_{am(270)}(\rho, \theta)$	$A_{am(270)}(\rho, \theta)+A_{am(360)}(\rho, \theta)$	Average	Stdev
7	AS-RMS	0.0034	0.0057	0.0141	0.0120	**0.0088**	0.0051
8	AS-ANGLE	81.15	83.15	75.30	73.30	78.23	4.68
9	As of Test Sample	$A_{am(0)}(\rho, \theta)-A_{am(90)}(\rho, \theta)$	$A_{am(90)}(\rho, \theta)-A_{am(180)}(\rho, \theta)$	$A_{am(180)}(\rho, \theta)-A_{am(270)}(\rho, \theta)$	$A_{am(270)}(\rho, \theta)-A_{am(360)}(\rho, \theta)$	Average	Stdev
10	AS-RMS	0.0321	0.0318	0.0291	0.0300	0.0308	0.0015
11	AS-ANGLE	36.15	38.15	30.30	28.30	33.23	4.68
12	Coma of System	$A_{am(0)}(\rho, \theta)+A_{am(180)}(\rho, \theta)$	$A_{am(90)}(\rho, \theta)+A_{am(270)}(\rho, \theta)$	$A_{am(180)}(\rho, \theta)+A_{am(360)}(\rho, \theta)$	Average	Stdev	
13	COMA-RMS	0.0008	0.0028	0.0015	**0.0017**	0.0010	
14	COMA-ANGLE	48.90	123.35	46.00	72.75	43.84	
15	Coma of Test Sample	$A_{am(0)}(\rho, \theta)-A_{am(180)}(\rho, \theta)$	$A_{am(90)}(\rho, \theta)-A_{am(270)}(\rho, \theta)$	$A_{am(180)}(\rho, \theta)-A_{am(360)}(\rho, \theta)$	Average	Stdev	
16	COMA-RMS	0.0138	0.0136	0.0138	0.0137	0.0001	
17	COMA-ANGLE	138.90	123.35	136.00	131.13	8.27	

Table 2 shows the calibrated RMS astigmatism and coma aberrations in λ, and direction angles in degree. The rows from 2 to 5 show the measured astigmatism and coma aberrations for the test sample being rotated by 90 degrees, 180 degrees, 270 degrees and 360 degrees. Shown in line 7, 8 and 13, 14 are astigmatism and coma aberrations of the system calculated according to Eq. (15) and (20). Shown in rows 10, 11 and 16, 17 are astigmatism and coma aberrations of the test sample calculated according to Eq. (18) and (22). Because the test lens is rotated by 90 degrees or 180 degrees several times, we can obtain average values and standard deviation of the calibrated RMS astigmatism and coma aberrations for the system and the test sample. It was found that the obtained systematic astigmatism and coma aberrations were 0.0088 λ and 0.0017 λ, respectively, which are about the same as those calibrated using the standard source described in the previous section.

6. Summary

A new wavefront measurement interferometer using reflection pinhole mirrors for generating reference wavefronts of different wavelengths is developed. The developed interferometer can be used for the measurement of wavefronts of focused or parallel multi-wavelength laser beams of BD (HD-DVD), DVD and CD pickups. The measurement results are in good agreement with those measured by a commercial FUJINON V10 interferometer. System errors are calibrated by a high precision standard source and the results of RMS astigmatism and coma aberrations are verified by estimation of data obtained by rotating the test sample by 90 degrees. The system can also be used for the measurement of objective lenses of optical pickups by using high precision standard sources, and parallel beams when the objective lens is removed from the pickup.

Acknowledgments

A part of this work was conducted at the AIST Nano-Processing Facility, supported by "Nanotechnology Network Japan" of the Ministry of Education, Culture, Sports, Science and Technology (MEXT), Japan.

#87937 - $15.00 USD Received 28 Sep 2007; revised 20 Nov 2007; accepted 23 Nov 2007; published 2 Jan 2008